

Improving engineering models of terramechanics for planetary exploration

A.J.R. Lopez-Arreguin^a, S. Montenegro^{b,*}

^a Institute of Space Systems, TU-Braunschweig, Hermann-Blenk-Strasse 23, Braunschweig, 38108, Germany

^b Informatik VIII, Universität Würzburg, Germany

ARTICLE INFO

Keywords:

Wheel
Terramechanics
Forces
Torque
Robotics

ABSTRACT

This short letter proposes more consolidated explicit solutions for the forces and torques acting on typical rover wheels, that can be used as a method to determine their average mobility characteristics in planetary soils. The closed loop solutions stand in one of the verified methods, but at difference of the previous, observables are decoupled requiring a less amount of physical parameters to measure. As a result, we show that with knowledge of terrain properties, wheel driving performance rely in a single observable only. Because of their generality, the formulated equations established here can have further implications in autonomy and control of rovers or planetary soil characterization.

Introduction

Planetary exploration

Key advances in space robotics have notable examples: science laboratories dropped in Mars or the Moon using wheeled rovers capable to do multi-disciplinary tasks while enduring extreme environments [1]. As planetary surfaces are covered by soils typically made out of regolith to bedrocks, rovers shall detect and avoid physically-visible obstacles using onboard sensors. But avoiding collisions with geological features is not the only hazard: most wheels can get stuck in the loose terrain if the rover mobility is not sensed accordingly. Thus, a lot of emphasis is focused onto the wheel-soil mechanics interaction, where the forces and torques acting on the center of mass of the wheels are representative. Many rovers also use grousers, which are protrusions or convex patterns on the wheels or tracks of vehicles that essentially improve their tractive effort. In the presence of such adapted wheel geometry, none of the well-known terramechanics model based on Bekker [2] and Wong [3] capture the dynamic effects arising in experimental measurements [4]. Further, the only expressions available in the literature, relate the wheel forces on diverse parameters that are difficult to measure in an actual rover commission (e.g. the multi-axis stresses [5]). Thus, deriving simplified forms of the forces/torques equations depending in a different set of more disposed parameters, can be a key for optimal tracking of the rover performance and avoid getting stuck in soils of low cohesion, as typical planetary surfaces. This is the purpose of this letter as will be related next.

Previous work

The progress of analytical terramechanics formulations are important to help in the design of better space hardware or for development of complex control laws for rovers. For instance, in the field of terramechanics the terrain parameters (e.g. bearing or shearing properties), wheel parameters (radius, width, lug number or lug geometry), wheel-terrain interaction parameters (e.g. combined rigidity coefficient, frictional coefficient), and motion state variables (slip ratio, contact angles and sinkage), are together employed to develop general mechanics models of wheel-terrain interaction (stresses and forces analytical expressions) [6]. Meanwhile the improvement of terramechanics models regarding stress formulations were formerly addressed in the well known Bekker's work [7], by Wong and Reece [5], and lately Shibly [8], Meirion [9] or Irani [4]. On the other hand, the progress on explicit force models have been much less developed recently. Only Iagnemma [10] and Shibly [8] adapted analytical close-form expressions from the classical terramechanics models for terrain parameter identification, while Ding et al. [11,12] developed explicit formulations that can be applied in the parametric design of optimal wheel radius and width according a given mass. From these previous authors, however, only the work of Ding seems to be robust enough to deal with complex slip-sinkage phenomenon as present in laboratory experiments. Further, the explicit solutions of the wheel forces and torques introduced in the literature, are often resolved in terms of highly coupled expressions and depending in a very large set of observables and fitting constants. Thus, in this short letter we stand on one of the verified equations of the macroscopic forces and

* Corresponding author.

E-mail address: amenosis.lopez@tu-braunschweig.de (S. Montenegro).

torques [11,12] acting over typical rover wheels with grousers, and derive a simplification that allows to track their time-characteristics in terms of one single motion state variable (the slip ratio) while reducing the number of fitting-related constants. The model can be also extrapolated to wheels with straight (plane) surfaces.

Normal and shear stress modeling

Let the normal wheel stress σ be formulated as a power-law function [2,6] in terms of sinkage z :

$$\sigma = K_s z^N \quad (1)$$

with K_s is the sinkage modulus representing a soil-strength parameter (characterized e.g. during pressure-sinkage tests), and $N = n_o + n_2 s$ is the sinkage exponent set in terms of fitting constants n_o and n_2 [11]. In the previous, s represents the wheel slip ratio:

$$s = \begin{cases} 1 - \frac{v_x}{r\omega} & \text{if driving} \\ \frac{r\omega}{v_x} - 1 & \text{if braking} \end{cases} \quad (2)$$

Hence, if the wheel lies static (not rotated), the slip would be zero, and the static sinkage would be $z = z_o$ while $N = n_o$. Since the wheel intrusion into the soil can be parametrized along the contact angle θ , we can demonstrate the sinkage in the wheel rear ($\theta_m \leq \theta \leq \theta_1$) is [3]:

$$z(\theta) = r(\cos\theta - \cos\theta_1) \quad (3)$$

where r is the wheel radius, θ_1 is the entry angle and θ_m the angle of maximum stress as displayed in Fig. 1(a). On the other hand, in the front region of the wheel ($\theta_2 \leq \theta < \theta_m$), sinkage can be given by [3]:

$$z(\theta) = r \cos \left[\theta_1 - \frac{\theta - \theta_2}{\theta_m - \theta_2} (\theta_1 - \theta_m) \right] - r \cos\theta_1 \quad (4)$$

Notice Eqs. (3) and (4) refer normal stresses are composed of two distribution functions along the wheel-soil interaction path. On the other hand, the shear stresses can be evaluated along the traveling direction (x-direction in Fig. 1(a)). The Janosi-Hanamoto is the standard formula to model τ_x :

$$\tau_x(\theta) = E[c + \sigma(\theta)\tan\phi] \quad (5)$$

where E is a function defined in terms of the soil shearing coefficient K :

$$E = 1 - \exp\left(-\frac{r}{K}\right)(\theta_1 - \theta - (1-s)(\sin\theta_1 - \sin\theta)) \quad (6)$$

Fig. 1(b) plots σ and τ_x using the previous models. The wheel dimensions are $r = 0.2\text{m}$ and $b = 0.1\text{m}$, covered with soil properties shown in the figure caption for sandy soil. Notice the distinct transition of the stress profiles between the forward and rearward regions of the wheel. In many cases, those can be approximated by linear functions [8,13] (for instance in typical natural terrains of low cohesion). Shibly et al. [8] derived the simplified stress equations in the following form:

$$\sigma_1(\theta) = \sigma_m \frac{\theta_1 - \theta}{\theta_1 - \theta_m} \quad (\theta_m \leq \theta \leq \theta_1) \quad (7a)$$

$$\sigma_2(\theta) = \sigma_m \frac{\theta - \theta_2}{\theta_m - \theta_2} \quad (\theta_2 \leq \theta \leq \theta_m) \quad (7b)$$

$$\tau_{1x}(\theta) = \tau_m \frac{\theta_1 - \theta}{\theta_1 - \theta_m} \quad (\theta_m \leq \theta \leq \theta_1) \quad (7c)$$

$$\tau_{2x}(\theta) = \tau_m \frac{\theta - \theta_2}{\theta_m - \theta_2} \quad (\theta_2 \leq \theta \leq \theta_m) \quad (7d)$$

In Eq. (7), τ_m and σ_m are the stresses evaluated at the angle θ_m , where the sinkage is:

$$z(\theta_m) \approx \frac{1}{2} z \quad (8)$$

with $z = z(t)$ the total sinkage measured at time t .

Force equations

Wheel forces and torques are the basic mean to evaluate the rover performance. In the case of wheel with straight surfaces (e.g. Fig. 1(a)), they can be integrated with knowledge of the multiple stresses acting on the differential wheel-soil contact area $r b d\theta$. In case the wheel incorporates grousers with a height h , as shown in Fig. 2, we must define an average shearing radius r_s where the stress τ can be considered to act [6]:

$$r_s = r + \lambda_s h \quad (9)$$

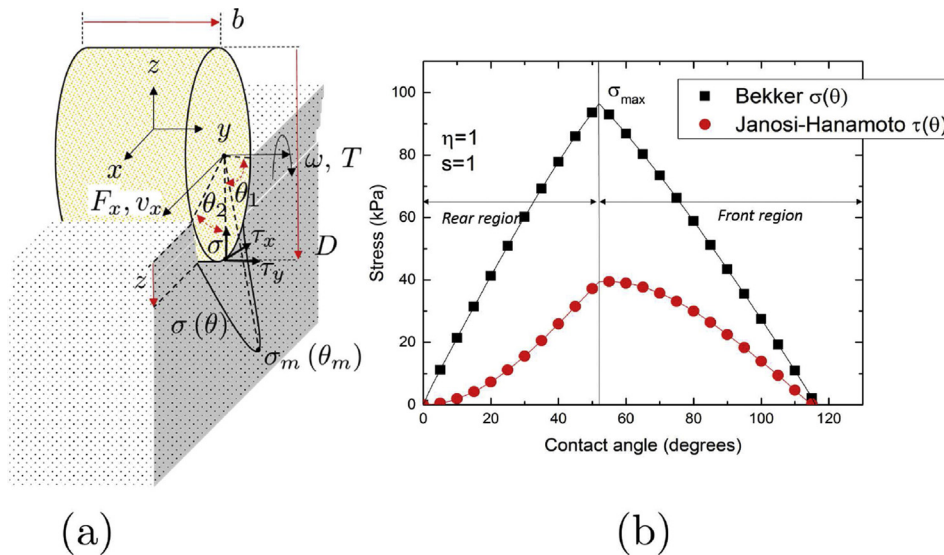


Fig. 1. (a) Basic terramechanics parameters set for a wheel with straight surfaces. (b) The plot of the normal stress distributions $\sigma(\theta)$ and shear stresses $\tau(\theta)$ for sandy soil. Here, soil constants are: $c = 0\text{ kPa}$, $\phi = 0.478\text{ rad}$, $n = 0.91$, $K = 0.005\text{ m}$, $k_c = -0.66 \frac{\text{kN}}{\text{m}^{0.91}}$ and $k_\phi = 754.13 \frac{\text{kN}}{\text{m}^{0.91}}$, from which $K_s = k_c/b + k_\phi$.

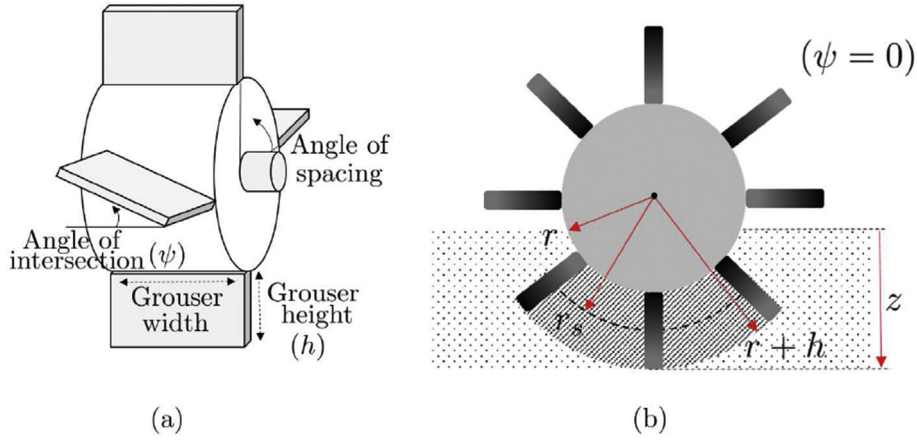


Fig. 2. The addition of lugs onto wheels allows to confere greater traction and improve the general rover performance. (a) Typical parameters of lugs. (b) Shearing radius definition, where $r_s = r + \lambda_s h$.

with λ_s is the lug coefficient, typically set to 0.5 [12]. The forces along the traveling direction and normal to the soil, as well as the torque now can be integrated explicitly:

$$F_x = r_s b \int_{\theta_2}^{\theta_1} [\tau_x(\theta) \cos\theta - \sigma(\theta) \sin\theta] d\theta \quad (10a)$$

$$F_z = r_s b \int_{\theta_2}^{\theta_1} [\tau_x(\theta) \sin\theta - \sigma(\theta) \cos\theta] d\theta \quad (10b)$$

$$T = r_s^2 b \int_{\theta_2}^{\theta_1} [\tau_x(\theta)] d\theta \quad (10c)$$

Typically, Eq. (10) is experimentally evaluated by multiple-axis force transducers mounted in the wheel or the testbed [14], or by measuring σ and τ_x along the contact path per rotation [15]. On the other hand, we can show with the linearized normal and shear stresses, forces and torques can be solved explicitly to obtain:

$$F_x = -B X + A Y \quad (11a)$$

$$F_z = A X + B Y \quad (11b)$$

$$T = r H Y \quad (11c)$$

In the previous, $X = r_s b \sigma_m$ and $Y = r_s b \tau_m$, while A and B are magnified constants that can be defined through [12]:

$$A = \frac{\cos\theta_m - \cos\theta_2}{\theta_m - \theta_2} + \frac{\cos\theta_m - \cos\theta_1}{\theta_1 - \theta_m} \quad (12a)$$

$$B = \frac{\sin\theta_m - \sin\theta_2}{\theta_m - \theta_2} + \frac{\sin\theta_m - \sin\theta_1}{\theta_1 - \theta_m} \quad (12b)$$

$$H = \frac{\theta_1 - \theta_2}{2} \quad (12c)$$

From above, the physical meaning of term AY is traction force provided by the wheel, while $-BX$ is the motion resistance exerted by the soil over the wheel center mass acting in the opposite direction of travel. Further, AX will represent the vertical force components due to normal stress, and BY the shear stress contribution along the same vertical axis. Also, $AX \gg BY$ if the wheel is static. It is now interesting to explore a simplification method for Eq. (12), that at difference from previous methods (e.g. Refs. [11,12]), can be decoupled relying on the sinkage or slip only. Because in soils of interest as in Mars or Lunar surface, the exit angle is very low [8], the entry angle can be approximated by:

$$\theta_1 = \frac{\arccos(1 - z/r)}{2} \quad (13)$$

Following, terms A and B from Eq. (12) can be expressed in relation to wheel parameters and fitting constants λ_A and λ_B [11]:

$$A \approx (1 - \lambda_A) \sqrt{\frac{z}{2r}} \quad (14a)$$

$$B \approx (1 + \lambda_B) \frac{z}{2r} \quad (14b)$$

From Eqs. (11), (12) and (14), we can immediately obtain the explicit solution for the longitudinal force:

$$F_x(t) = - (1 + \lambda_B) b K_s \left(\frac{z(t)}{2}\right)^{N(t)+1} + r_s \sqrt{r} (1 - \lambda_A) b E K_s \tan\phi \left(\frac{z(t)}{2}\right)^{N(t)+\frac{1}{2}} + r_s \sqrt{r} (1 - \lambda_A) b E c \left(\frac{z(t)}{2}\right)^{\frac{1}{2}} \quad (15)$$

Eq. (15) reflects that F_x can be mapped with knowledge of all soil-related parameters (K_s , E , ϕ , c), thus only requiring time measurements of the sinkage and slip (hence N can be determinable as derived before). Similarly, the normal force would depend in the same observables as above:

$$F_z(t) = \frac{r_s}{r} (1 + \lambda_B) b E K_s \tan\phi \left(\frac{z(t)}{2}\right)^{N(t)+1} + \sqrt{r} (1 - \lambda_A) b K_s \left(\frac{z(t)}{2}\right)^{N(t)+\frac{1}{2}} + \frac{r_s}{r} (1 + \lambda_B) b E c \left(\frac{z(t)}{2}\right) \quad (16)$$

Finally, the torque explicit formula relies in less constants than for previous forces:

$$T(t) = \frac{r_s^2}{2} b E \arccos\left(1 - \frac{z(t)}{r}\right) \left[c + \left(\frac{z(t)}{2}\right)^{N(t)} K_s \tan\phi \right] \quad (17)$$

It is interesting to note, how previous formulations can be derived through slip and sinkage measurements in time. However, it would be desirable to rely only on a single variable only (e.g. the slip), as sinkage estimation is not straightforward (we would need onboard cameras and imaging processing techniques [16,17]). Thus, the sinkage variation in time can be approximated through [18]:

$$z(t) = \frac{1 + s}{1 - 0.5 s} z_0 \quad (18)$$

where z_0 is the static sinkage. Finally, in previous work explicit solutions of the longitudinal or normal forces were addressed as function of the torque (or viceversa) with highly coupled equations, and the experiments showed an overall good compromise in the results with a low relative error (in general of less than 4.13%) [12]. The expressions presented here were derived using experimentally-verified solutions for the magnified constants (Eq. (14)), that allow us to resolve F_x , F_z and T equally as only function of the sinkage, wheel and terrain parameters, and some fitting constants. Thus, the newer expressions introduced (Eqs. 15–17) may be fundamental for further applications in the domain of in-situ detection of forces or torques given few rover observables.

Conclusion

We shown that wheel forces in low cohesion soils can attain new explicit solutions related to soil constants and only the sinkage or slip evolution. Because none of the previous authors have placed emphasis in derive the equations decoupled, here we first note only one observable is required to compute the longitudinal force, thus avoiding the typical process of numerical integration of the stress distributions. Also, most researchers use of force/torque transducers which are inherently complex to instrument in actual rovers, hence attaining large complexity to perform terramechanical studies, that can be advantaged by tracking the slip alone with the method proposed above. Further, since the vertical force can be easily inferred by a rover (e.g. kinematic analysis of the suspension [8]), the formula can be used for soil parameter identification, in order to characterize some of the terrain constants. Finally, as the previous equations can account for lugged wheels, the dynamic oscillations typically observed for this rigid models are not accounted, although the equations derived typically represent the mean of the fluctuations in general [4].

Conflict of interest

The authors declare that they have no competing interests.

Acknowledgements

This publication was funded by the German Research Foundation (DFG) and the University of Wuerzburg in the funding programme Open

Access Publishing.

References

- [1] S. Chhaniyara, C. Brunskill, B. Yeomans, M. Matthews, C. Saaj, S. Ransom, et al., Terrain trafficability analysis and soil mechanical property identification for planetary rovers: a survey, *J. Terramechanics* 49 (2) (2012) 115–128.
- [2] M.G. Bekker, *Theory of Land Locomotion*, University of Michigan Press, 1956.
- [3] J.Y. Wong, *Theory of Ground Vehicles*, John Wiley & Sons, 2001.
- [4] R. Irani, R. Bauer, A. Warkentin, A dynamic terramechanic model for small lightweight vehicles with rigid wheels and grousers operating in sandy soil, *J. Terramechanics* 48 (4) (2011) 307–318.
- [5] J.Y. Wong, A. Reece, Prediction of rigid wheel performance based on the analysis of soil-wheel stresses part i. performance of driven rigid wheels, *J. Terramechanics* 4 (1) (1967) 81–98.
- [6] L. Ding, Z. Deng, H. Gao, J. Tao, K.D. Iagnemma, G. Liu, Interaction mechanics model for rigid driving wheels of planetary rovers moving on sandy terrain with consideration of multiple physical effects, *J. Field Robot.* 32 (6) (2015a) 827–859.
- [7] M.G. Bekker, *Off-the-road Locomotion: Research and Development in Terramechanics*, University of Michigan Press, 1960.
- [8] H. Shibly, K. Iagnemma, S. Dubowsky, An equivalent soil mechanics formulation for rigid wheels in deformable terrain, with application to planetary exploration rovers, *J. Terramechanics* 42 (1) (2005) 1–13.
- [9] G. Meirion-Griffith, C. Nie, M. Spenko, Development and experimental validation of an improved pressure-sinkage model for small-wheeled vehicles on dilative, deformable terrain, *J. Terramechanics* 51 (2014) 19–29.
- [10] K. Iagnemma, H. Shibly, S. Dubowsky, On-line terrain parameter estimation for planetary rovers, in: *Proceedings 2002 IEEE International Conference on Robotics and Automation* (Cat. No. 02CH37292), vol. 3, IEEE, 2002, pp. 3142–3147.
- [11] L. Ding, et al., Improved explicit-form equations for estimating dynamic wheel sinkage and compaction resistance on deformable terrain, *Mech. Mach. Theory* 86 (2015b) 235–264.
- [12] L. Ding, K. Yoshida, K. Nagatani, H. Gao, Z. Deng, Parameter identification for planetary soil based on a decoupled analytical wheel-soil interaction terramechanics model, in: *2009 IEEE/RSJ International Conference on Intelligent Robots and Systems*, IEEE, 2009, pp. 4122–4127.
- [13] K. Iagnemma, S. Kang, H. Shibly, S. Dubowsky, Online terrain parameter estimation for wheeled mobile robots with application to planetary rovers, *IEEE Trans. Robot.* 20 (5) (2004) 921–927.
- [14] L. Ding, H. Gao, Z. Deng, K. Nagatani, K. Yoshida, Experimental study and analysis on driving wheels' performance for planetary exploration rovers moving in deformable soil, *J. Terramechanics* 48 (1) (2011) 27–45.
- [15] S. Higa, K. Sawada, K. Nagaoka, K. Nagatani, K. Yoshida, Three-dimensional stress distribution on a rigid wheel surface for a lightweight vehicle, in: *Proceedings of the 13th European Conference of the ISTVS*, 2015, pp. 383–391.
- [16] C.A. Brooks, K.D. Iagnemma, S. Dubowsky, Visual wheel sinkage measurement for planetary rover mobility characterization, *Aut. Robots* 21 (1) (2006) 55–64.
- [17] Y. Gao, C. Spiteri, C.L. Li, Y.C. Zheng, Lunar soil strength estimation based on chang'e-3 images, *Adv. Space Res.* 58 (9) (2016) 1893–1899.
- [18] M. Lyasko, Slip sinkage effect in soil-vehicle mechanics, *J. Terramechanics* 47 (1) (2010) 21–31.